

Analysis of Induced-radioactivity using DCHAIN-SP for Pb and Hg at a Mercury Target Irradiated by 2.8 and 24 GeV Protons

Yoshimi Kasugai, Tetsuya Kai, Fujio Maekawa, Shinichiro Meigo, Hiroshi Takada, Yujiro. Ikeda

Japan Atomic Energy Agency
Tokai-mura, Naka-gun, Ibaraki-ken 319-1195
e-mail: kasugai.yoshimi@jaea.go.jp

The high energy particle induced radioactivity calculation code system consisting PHITS, MCNP4C and DCHAIN-SP 2001 was validated for mercury and lead samples by the experimental activation data obtained using AGS (Alternative Gradient Synchrotrons) accelerator at Brookhaven National Laboratory. As a result, we found that the calculation is consistent with the experimental data within a factor of 2 on the average. Mass yield curves of the spallation reactions were approximately deduced using the experimental activation data.

1. Introduction

Radioactivity estimation in spallation neutron field including incident high-energy protons is essential for designing spallation neutron target and accelerator driven nuclear transmutation system. In particular, the estimation for heavy material such as mercury and lead is important since those elements are used as target materials. However, the radioactivity estimation for such heavy material has not been easy and reliable, because the products cover wide range of nuclei, consideration of huge kinds of reaction paths is required, and the most of reaction cross sections for high energy incident particles are unknown or unreliable.

A radioactivity calculation code consisting PHITS, MCNP4C and DCHAIN-SP 2001 [1] has been used for the radioactivity estimation for design of the J-PARC facilities. It is important to know the safety margin of the calculation code for efficient and reliable design. The code validation has been carried out using the experimental activation data for 14 MeV neutron field, and the nuclide production calculation by PHITS has been validated using the experimental cross section data in literature. However the code validation for mixed radiation field including incident protons and spallation neutrons has not been performed yet. Therefore, we carried out the activation experiment for such kinds of mixed field using AGS (Alternative Gradient Synchrotrons) accelerator at Brookhaven National Laboratory. Using these data, we validated the code system for the major structural materials irradiated in the mixed radiation field. In this paper, we present the analytical results for mercury and lead samples.

2. Experiment

Schematic drawing of the AGS accelerator complex and the mercury target used in the experiment are shown in Figs. 1 and 2, respectively. In the experiment, the samples of mercury-oxide, lead and others were irradiated around the mercury target, which was bombarded with 2.83 and 24 GeV protons. The samples were placed at the top and side of the target; the top and side samples were called "On-" and "Off-beam" samples, respectively. The on-beam samples were irradiated by incident protons in addition to secondary neutrons, and the off-beam samples were mainly irradiated by the spallation neutrons from the target. The number of protons injected to each on-beam sample were determined by the foil activation method using the reference reaction of $\text{Cu}(p, x)^{24}\text{Na}$. Using the previous experimental data, the cross section values were evaluated to be 3.5 ± 0.5 mb and 3.5 ± 0.2 mb at the proton energies of 2.83 GeV and 24 GeV, respectively. The total incident protons were measured by an integrating current transformer (ICT) and separated electron chamber (SEC). The neutron flux at the off-beam samples were validated using $^{93}\text{Nb}(n, 2n)^{92\text{m}}\text{Nb}$ reaction. After the irradiation, the radioactivities of samples were measured with HPGe detectors at the cooling time between 2 h and 267 d. The detail of the experimental procedure and

the experimental data were shown in the reference [2].

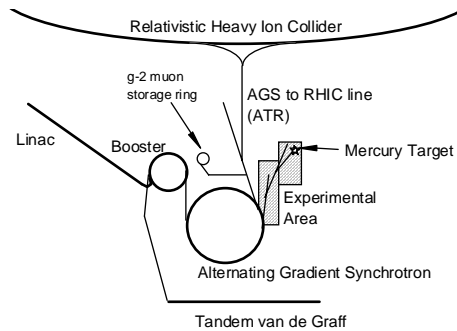


Fig. 1 A schematic drawing of the AGS accelerator complex.

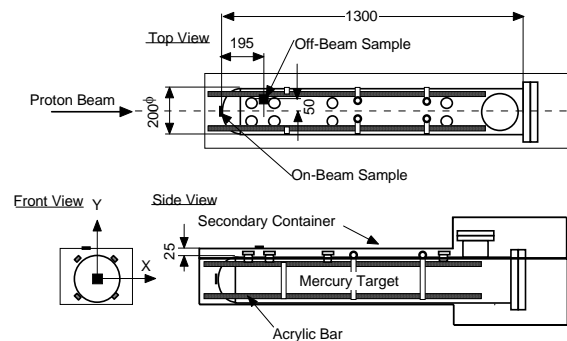


Fig. 2 Top, front and side view of the mercury target. The target container was made of stainless steel with 2.5 mm in thickness. The acrylic bar was used to set the activation detectors for measurement of neutron performance of the mercury target.

3. Analysis

In the analysis, we used the calculation model including the mercury target, a target container of stainless steel, all samples and concrete walls of the irradiation room. Proton beam profile was assumed to be a Gaussian distribution which was measured parameters of a full width at half maximum (FWHM) and the center of proton beam. For each sample, proton spectrum was calculated by PHITS, and neutron spectrum was obtained by PHITS (>20 MeV) and MCNP/4C(<20 MeV). Using the proton energy spectra and the neutron energy spectra above 20 MeV, nuclear production yields were calculated by PHITS. DCHAIN-SP calculated the radioactivity of the samples by using the nuclear production yields and the neutron energy spectra below 20 MeV. For the off-beam samples, the proton energy spectra were normalized to the number of protons obtained by the activation method using the copper foil. The proton energy spectra of the samples on the side surface and the neutron energy spectra were normalized to the number of incident protons measured by ICT. The calculation procedure is described in the reference presented in this conference [3].

4. Result and Discussion

Decay curves of induced radioactivities were calculated for each sample. Figure 3 shows the calculated decay curves and the experimental data for mercury-oxide samples irradiated at on-beam position for 2.83 GeV protons. This figure shows that the calculation well-reproduces the decay feature of major products such as ^{203}Hg , $^{197\text{m}}\text{Hg}$, $^{198\text{g}}\text{Au}$, ^{185}Os and $^{182\text{m}}\text{Re}$. C/E-values for each radioactive product are shown for mercury-oxide and lead samples in Fig. 4 and 5, respectively. If we had multiple

experimental data with different cooling time, the average values were adopted as representative values. These figures show that the calculation is consistent with the experimental data within a factor of 2 on the average. However, the calculated values are lower than the experimental data on the whole. In addition the C/E-values have the mass-number dependence, which implies that the calculated yield curve for spallation reactions shows different tendency from the real curve. In order to make it clear, the experimental-basis mass yield curves for Pb were deduced under the assumptions as follows:

- Proton-number (Z) dependence of calculated spallation yield at a fixed mass number (A) is approximately reasonable.
- The differences between the calculated and experimental radioactivities are largely due to the calculated mass yield.

On the basis of these assumptions, the experimental-basis mass yields were deduced from (Calculated total yield)/(C/E). The upper figures in Fig. 6 show the mass yield curves for Pb samples irradiated at on-beam position on 2.83 and 24 GeV incident protons. The calculated production yield for proton- and neutron-incidents and the total yield curves are shown in the figure. The lower figures show the C/E-values for radioactivities as a function of mass number of products. Experimental-basis yields are shown by circles in the upper figures. Considering the distribution of the circles, the yield curves should be drawn in between the two dotted lines indicated by two-headed arrows in order to obtain more consistency between the calculation and the experimental data. The calculation curves at $A \sim 20$ and 170 show underestimation by a factor of more than 10 and 2, respectively.

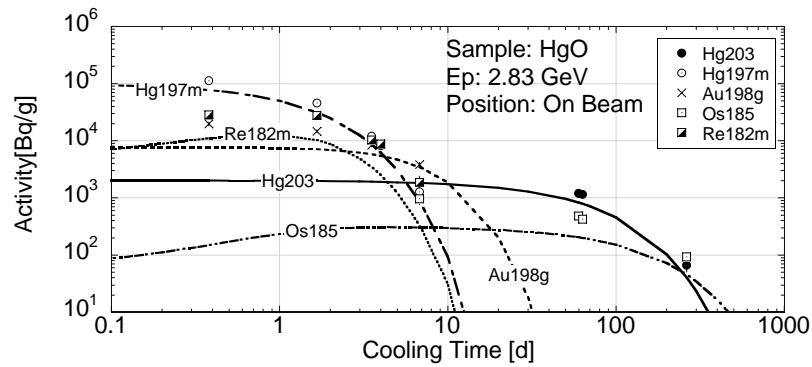


Fig. 3 Radioactivity of the HGO sample irradiated at on-beam position for 2.83 GeV incident protons. Circles, squares and crosses show the measured data, and lines show the decay curve calculated using DCHAIN-SP.

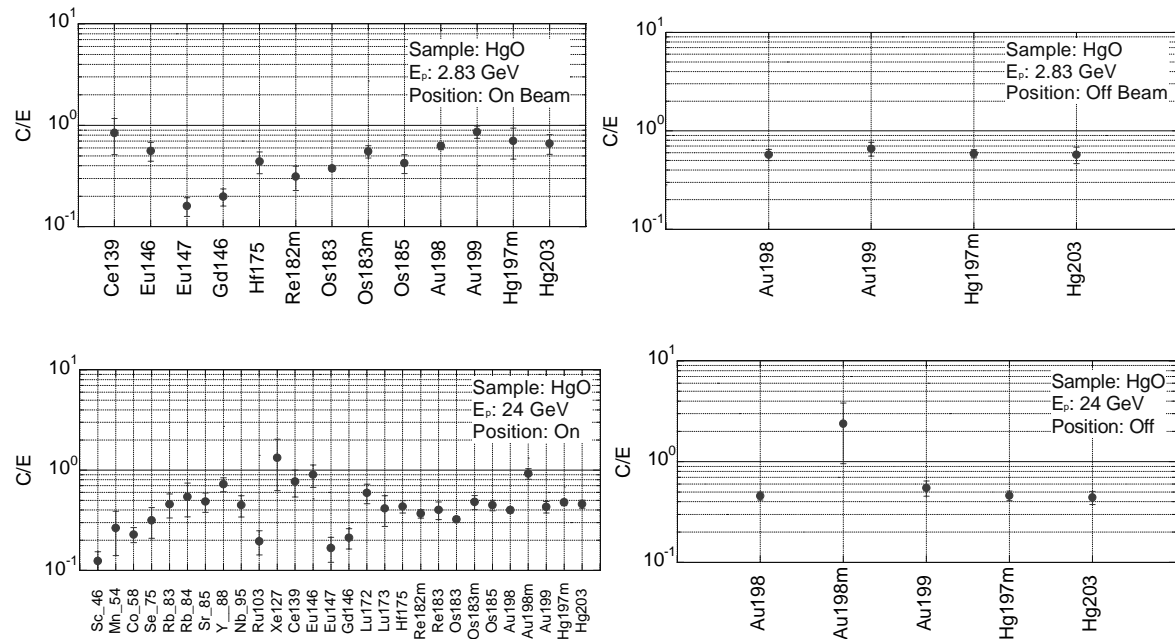


Fig. 4 C/E for the radioactivity of HgO samples.

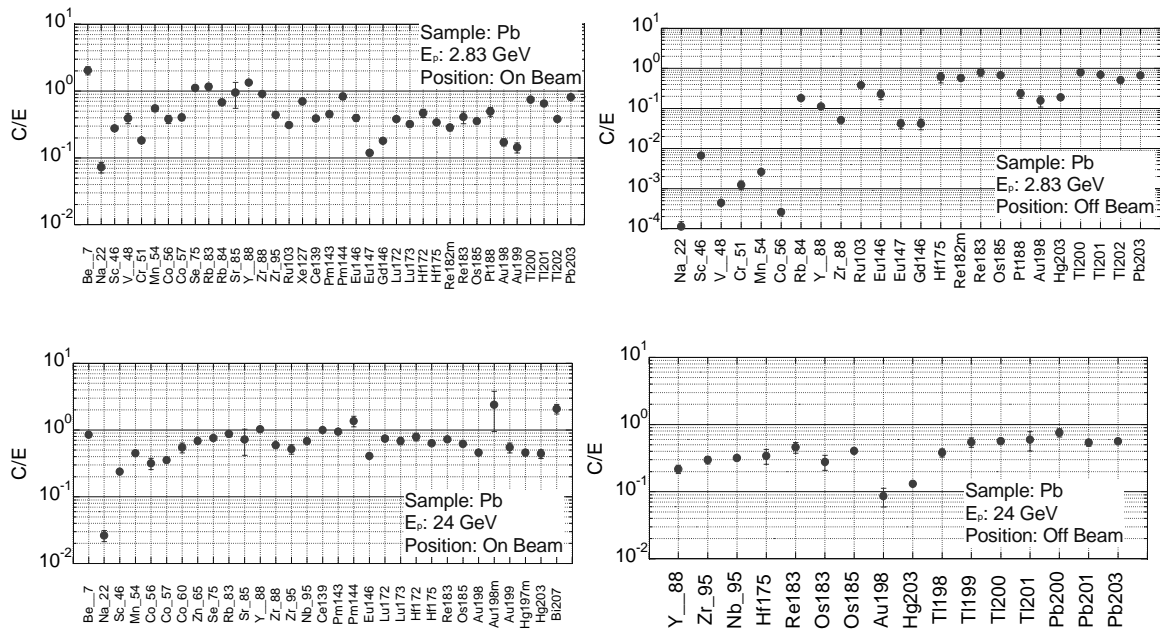


Fig. 5 C/E for the radioactivity of Pb samples.

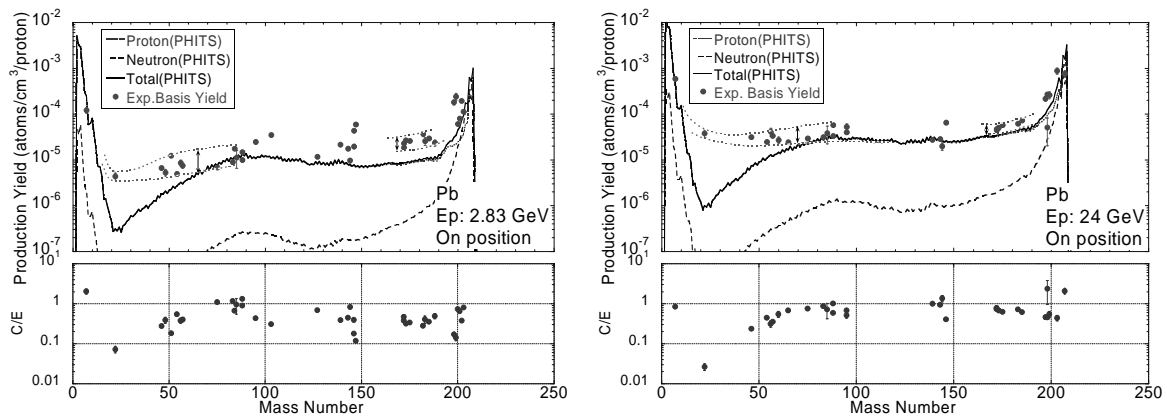


Fig. 6 The upper figures show the mass yield curves for the Pb sample irradiated at on-beam position on 2.83 and 24 GeV incident protons. In the figures the dotted lines show the production yield for protons and neutrons, and the solid lines show the total yield curve. The lower figures show the C/E values of radioactivities as a function of mass number of products. The closed circles in the upper figures are experimental-basis yield deduced by dividing the calculated total yield by the C/E-value. On the basis of the present experimental data, the yield curves should be drawn in between the two dotted lines indicated by two-headed arrows.

In order to check the calculation in detail, proton-induced cross sections for 2.8 and 24 GeV were estimated using the present activation data of the on-beam samples by neglecting the contribution of neutrons. Since the radioactive products in the on-beam samples were almost induced by incident protons except at $A \sim 200$, we supposed to obtain the reasonable proton-induced cross sections using the present activation data. In Fig. 7, the cross sections deduced using the present data are plotted as a function of the mass number of products. Previous reported data of Gloris et al. [4] for 1.6 GeV protons are shown in the figure for reference. The mass-yield cross sections calculated by PHITS were also plotted. At $A \sim 170$, the Gloris' data for 1.6 GeV shows 20~30 mb and the present data for 2.83 and 24 GeV are 20~30 mb and 10~20 mb, respectively. The present values are reasonable considering the typical shape of the excitation curves in this mass region. The experimental cross sections, which is cumulative yields of spallation products, can be interpreted as the minimum value of the mass yield cross section. The mass yield curve should always be larger than the experimental data. In this context, the calculation curve of PHITS shows

underestimation at $A \sim 20$ and 170.

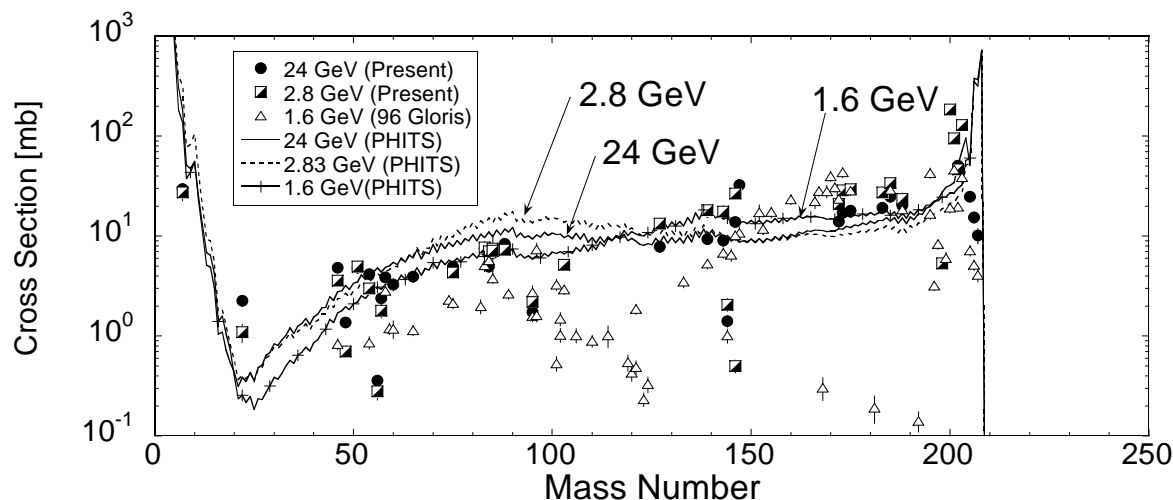


Fig. 7 Proton induced cross sections for 2.8 and 24 GeV were deduce using the present experimental data for the on-beam samples by neglecting the contribution of neutrons. The closed and open circles show the present data for 24 and 2.83 GeV protons, respectively. The experimental data for 1.6 GeV protons, which were reported by Gloris et al.[4], are plotted by triangles. The lines show the calculation curves by PHITS for 1.6, 2.83 and 24 GeV incident-protons.

5. Summary

The high energy particle induced radioactivity calculation code system was validated for mercury and lead samples by using the experimental activation data. As a result, the calculation is consistent with the experimental data within a factor of 2 on the average, and calculated values are lower than the experimental data on the whole. Mass yield curves of the spallation reactions could be approximately deduced using the experimental activation data. By comparing between the experimental-basis mass yield curve and the calculation curve, we found that the calculation show underestimation by a factor about 2 around $A \sim 170$. The calculated production yield should be larger by a factor more than 10 at $A \sim 20$.

Acknowledgements

The authors would like to thank Drs. K. Niita, C. Konno and T. Katoh for their useful comment.

References

- [1] T. Kai, F. Maekawa, K. Kosako, Y. Kasugai, T. Takada and Y. Ikeda: "DCHAIN-SP 2001: High Energy Particle Induced Radioactivity Calculation Code", JAERI-Data/Code 2001-016 (2001) (In Japanese).
- [2] Y. Kasugai, T. Kai, F. Maekawa, H. Nakashima, H. Takada, C. Konno, M. Numajiri, T. Ino and K. Takahashi: "Measurement of Radioactivity induced by GeV-Protons and Spallation Neutrons using AGS Accelerator.", JAERI-Research 2003-034 (2004).
- [3] T. Kai, Y. Kasugai, F. Maekawa, S. Meigo, H. Takada, Y. Ikeda: "Analysis of Induced-radioactivity using DCHAIN-SP for Light Nuclei at a Mercury Target Irradiated by 2.8 and 24 GeV Protons", in this proceedings.
- [4] M. Gloris, R. Michel, U. Herpers and F. Sudbrock and F. Filges: Nucl. Instrum. and Methods, B113, 429 (1996).